12-1-2008

Rainbows in the Grass. II. Arbitrary Diagonal Incidence

Charles L. Adler

James A. Lock
Cleveland State University, j.lock@csuohio.edu

Richard W. Fleet

Original Citation

Adler, Charles L., James A. Lock, and Richard W. Fleet. "Rainbows in the Grass. II. Arbitrary Diagonal Incidence." *Applied Optics* 47 (2008): H214-H219.

Rainbows in the grass. II. Arbitrary diagonal incidence

Charles L. Adler,[1,*] James A. Lock,[2] and Richard W. Fleet[3]

[1]Department of Physics, St. Mary's College of Maryland, St. Mary's City, Maryland, 20618

[2]Department of Physics, Cleveland State University, Cleveland, Ohio, 44115

[3]Newbury Astronomical Society, Newbury, Berkshire RG14 7TZ, UK

*Corresponding author: cladler@smcm.edu

Received 21 May 2008; accepted 18 June 2008;
posted 8 September 2008 (Doc. ID 96528); published 21 November 2008

We consider external reflection rainbow caustics due to the reflection of light from a pendant droplet where the light rays are at an arbitrary angle with respect to the horizontal. We compare this theory to observation of glare spots from pendant drops on grass; we also consider the potential application of this theory to the determination of liquid surface tension.

OCIS codes: 010.7340, 290.0290.

1. Introduction

In a companion paper in this issue we considered the fold, or rainbow, caustic due to the reflection of light from a pendant droplet [1]. The caustic comes about because of the existence of an inflection circle near the neck of the droplet where the Gaussian curvature of the droplet vanishes [2]. In that paper we considered the case in which horizontal light rays were incident on a droplet that was radially symmetric in the horizontal plane, and we showed good agreement between theory and observations of pendant drops created in the laboratory. In particular, the shape of the caustic depended sensitively on the opening angle of the tangent cone at the inflection circle; if the tangent cone angle was greater than $\pi/4$ (45°), the rainbow caustic started at forward scattering and did not extend to scattering angles of π (180°), but instead curved back; if the tangent cone was smaller, it did extend to those angles [1]. However, this theory is not applicable to naked-eye observations of natural pendant droplets on grass that are created by dew or guttation, since they are not illuminated by light that is horizontally incident; indeed, the observations of these naturally occurring rainbows in the grass occurs in late morning, where the solar angle is typically ~40° at scattering angles $\varphi \sim 90°$.

Here we develop a theory of external reflection rainbows in which the incident light is at an arbitrary diagonal incidence angle. There is still one significant restriction of our theory in that we assume that the attachment of the droplet to the blade of grass is perfectly flat; that is, we assume that the plane to which the droplet is attached is perfectly flat and horizontal. We do not think that this is too severe a restriction of our theory in that the generic shape of the caustic will be preserved under small distortions of the droplet shape [3]. We also consider the application of the ideas developed in this paper for liquid diagnostics, namely, the determination of droplet surface tension and macroscopic contact angle.

2. Theory

Figure 1 shows the glare spot due to a pendant droplet in the garden of one of the authors, while Fig. 2 shows an out-of-focus image of the glare spot with the Airy fringes of the reflection caustic. Note that the glare spot occurs near the circle of inflection on the droplet where the droplet shape goes from convex to concave. By way of contrast, Fig. 3 shows the specular reflection of the Sun from the droplet at a point distant from the inflection circle, while Fig. 4 shows the out-of-focus image of it; no fringes are seen, showing clearly that the reflection is not a caustic. Figure 5

0003-6935/08/34H214-06$15.00/0

Fig. 1. (Color online) Droplet with reflected glare spot.

shows the geometry of the droplet in the region of the inflection circle and the incident light beam; in particular, ψ is the angle that the incident light rays make with the horizontal, and θ and ϕ are the azimuthal and polar angles of the reflected light ray, respectively. We refer the reader to Subsections 2.A and 2.B and Figs. 3, 4, and 5 of [1] for the mathematical development of the geometry of the problem. We develop the theory in this paper in two subsections: we consider, first, the caustic due to diagonally incident light grazing the droplet near the inflection circle and, second, the caustic due to light at an arbitrary diagonal incidence.

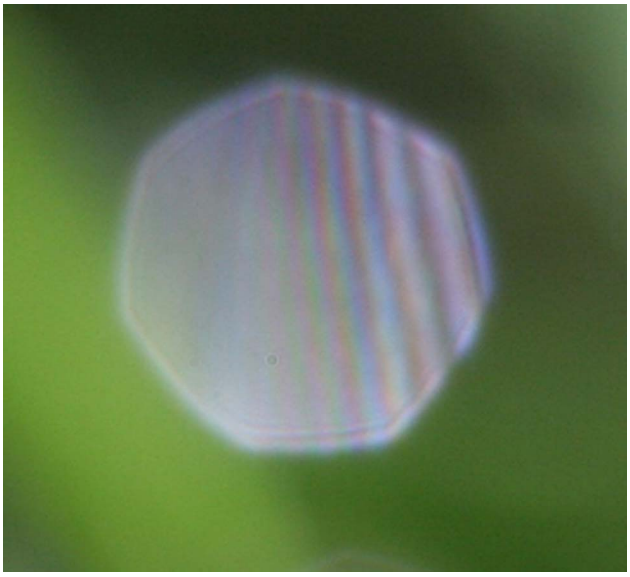

Fig. 2. (Color online) Out-of-focus image of the glare spot from Fig. 1, showing Airy fringes.

Fig. 3. (Color online) Specular reflection of sunlight from the body of a droplet.

A. Grazing Diagonal Incidence

The ray theory derivation of the argument of the Airy caustic of [1] may be repeated when the incoming plane wave is diagonally incident on the droplet as in Eq. (4) of [1] with $\psi \neq 0$. A number of new considerations occur for diagonal incidence that did not occur for horizontal incidence. First, the portion of the droplet illuminated by the beam now begins at the angle ϵ in the horizontal plane with

$$\sin(\epsilon_{\min}) = -\tan(\xi)\tan(\psi) \tag{1}$$

rather than at $\epsilon = 0$ as was the case for horizontal incidence, where ξ is the opening half-angle of the tangent cone. Thus more than half of the droplet circumference is illuminated when $\psi > 0$ and less than half is illuminated when $\psi < 0$. Near-grazing incident rays are now conveniently parameterized by Δ, where

$$\sin(\epsilon) = -\tan(\xi)\tan(\psi) + \Delta/\cos(\psi) \tag{2}$$

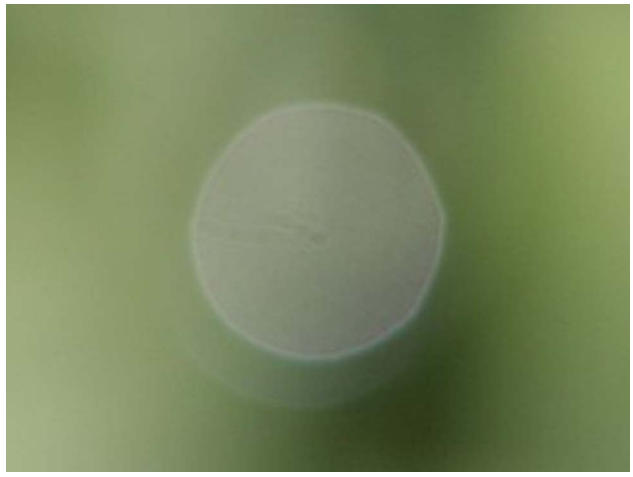

Fig. 4. (Color online) Out-of-focus image of the reflection in Fig. 3. Note the absence of interference fringes.

and $\Delta \ll 1$. The laboratory xyz coordinate system has the z axis coinciding with the symmetry axis of the droplet, and the x axis is positioned so that the propagation direction of the incident light rays is in the xz plane. Next, another coordinate system x', y', z' is formed by rotating the original x, y, z coordinate system through the angle ψ in the xz plane so that the x' direction coincides with the direction of the incoming light. The spherical coordinate angles Θ' and Φ' in this new coordinate system are defined with respect to the x' direction so that

$$\tan(\Phi') = (k_{\text{ref}})_{z'}/(k_{\text{ref}})_{y'}, \tag{3}$$

where $\mathbf{k}_{\text{ref}}$ is the direction of the reflected light and

$$\Theta' \approx \tan(\Theta') = [(k_{\text{ref}})_{y'^2} + (k_{\text{ref}})_{y'^2}]^{1/2}/(k_{\text{ref}})_{x'}. \tag{4}$$

The angular position (Θ', Φ') of a point on the rainbow on a far-zone viewing screen normal to the x' axis a distance R from the droplet, corresponding to the input parameters $\epsilon \geq \epsilon_{\min}$ on the inflection circle and $\delta = 0$, is

$$\Phi' = \Phi_0{}' - \Theta' \sin(\psi)/2D^2, \tag{5}$$

$$\Theta' = 2\Delta \times \cos(\xi), \tag{6}$$

where

$$D^2 = \cos^2(\xi)\cos^2(\psi) - \sin^2(\psi)\sin^2(\psi), \tag{7}$$

$$\tan(\Phi_0{}') = \sin(\xi)/D. \tag{8}$$

For diagonal incidence with the angle ψ, the rainbow due to near-grazing incidence rays on the far-zone viewing screen normal to the x' axis is curved, rather than being straight as was the case in [1] for $\psi = 0$. The rainbow curves downward from the $\Phi = \Phi_0{}'$ line if $\psi > 0$, and it curves upward from the $\Phi = \Phi_0{}'$ line if $\psi < 0$. The curvature of the rainbow caustic will be treated in more detail in Subsection 2.B.

Consider a point $(\Theta_R{}', \Phi_R{}')$ on the rainbow as seen on the viewing screen corresponding to the input parameters Δ_R on the inflection circle and $\delta = 0$. Construct the normal to the rainbow curve at that point, and traverse a distance σ' along the normal on the viewing screen away from the rainbow, where

$$\sigma' = R\Theta'\Gamma'. \tag{9}$$

The end of the traverse will be called point S. The spherical coordinates of S are found to be

$$\tan(\Phi_S{}') = \tan(\Phi_R{}') - \Gamma'/\cos^2(\Phi_R{}'), \tag{10}$$

$$\Theta_S{}' = \Theta_R{}'[1 - \Gamma'\Delta \times \cos(\xi)\sin(\psi)\cos^2(\psi)\cos^2(\Phi_R{}')/D^3]. \tag{11}$$

The two rays that reflect from the droplet surface and interfere at point S on the normal line correspond to the input ray parameters Δ_S and $\pm\delta_S$ above or below the inflection circle, where

$$\delta_S{}^2 = \Gamma' D/[3\alpha \times \cos^3[\xi]], \tag{12}$$

$$\Delta_S = \Delta_R + \Gamma' \sin(\psi) D/\cos^3(\psi). \tag{13}$$

Contrary to the case of normal incidence, we now have $\Delta_S > \Delta_R$.. The path length difference of the $(\Delta_S, \pm\delta)$ rays is then calculated after much algebra to be

$$\Delta_{S_{\text{total}}} = 8\alpha\delta^3\Delta_S \cos(\xi). \tag{14}$$

Equation (14) is then written in terms of the radial distance ρ' on the viewing screen, where

$$\rho' = R\Theta' \tag{15}$$

and the distance σ' is normal to the rainbow. The path length difference of the two interfering rays is then identified with the asymptotic form of the Airy integral. One finally obtains

$$E_{\text{total}}(\rho, \sigma) \approx \text{Ai}\{-k^{2/3}\sigma' D/[3^{1/3}\alpha^{1/3}R^{1/3}\rho'^{1/3}\cos^{7/3}(\xi)]\} \tag{16}$$

as the form of the reflection rainbow for diagonally incident near-grazing rays. As expected, Eq. (16) reduces to Eq. (21) of [1] in the $\psi \to 0$ limit.

B. Arbitrary Diagonal Incidence

In this section we consider arbitrary diagonal incidence with $\psi \neq 0$ and $\epsilon_{\min} \leq \epsilon \leq \pi/2$. Since the incident wavefront is tilted with respect to the xz plane, a ray on the incident wavefront is parameterized by its horizontal distance b' from the $-x'$ axis and its height z' above the $x'y'$ plane. The surface of the cone is given (as in [1]) by

$$r_0 = a - z_0 \tan(\xi), \tag{17}$$

where the subscript 0 denotes a position on the cone surface. The ray with

$$b' = 0, \qquad z' = z'_{\max} = aA \cos(\psi)\cos(\xi)/\sin(\xi) \tag{18}$$

with

$$A = 1 + \tan(\psi)\tan(\xi) \tag{19}$$

is incident at the apex of the cone. For $z' < z'_{\max}$, the grazing incident ray is parameterized by

$$b' = b'_{\max} = a(A/B)^{1/2}(1 - z'/z'_{\max}) \tag{20}$$

with

$$B = 1 - \tan(\psi)\tan(\xi). \tag{21}$$

We define the parameter Ω as

$$\Omega = \sin(\epsilon)\cos(\psi) + \sin(\xi)\sin(\xi). \tag{22}$$

Here Ω corresponds to the progression from grazing incidence to head-on incidence, the scattering angles of the reflected rays shown in Fig. 5 are

$$\sin(\phi) = 2\Omega\ \sin(\xi) - \sin(\psi), \tag{23}$$

$$\begin{aligned}\cos(\theta) = [\cos^2(\psi) + 2\Omega\ \times \sin(\psi\ \times \sin(\xi) - 2\Omega^2]/\\ \{\cos(\psi)[\cos^2(\psi) + 4\Omega \times\ \sin(\psi)\sin(\xi)\\ - 4\Omega^2\sin^2(\xi)]^{1/2}\}.\end{aligned} \tag{24}$$

The $\psi \to 0$ limit of Eqs. (23) and (24) are Eqs. (27) and (28) in [1]. The trajectory of the principal peak of the Airy caustic on the cylindrical viewing screen is

$$\begin{aligned}&-\psi \le \phi \le 2\xi - \psi\\ &\text{if } \xi \le \pi/4 + \psi/2, -\psi \le \phi \le \pi - 2\xi - \psi\\ &\text{if } \xi > \pi/4 + \psi/2,\end{aligned} \tag{25}$$

$$\begin{aligned}&0 \le \theta \le \pi \quad \text{if } \xi < \pi/4 + \psi/2, 0 \le \theta \le \pi/2\\ &\text{if } \xi = \pi/4 + \psi/2, 0 \le \theta \le \theta_{\max} \quad \text{if } \xi > \pi/4 + \psi/2,\end{aligned} \tag{26}$$

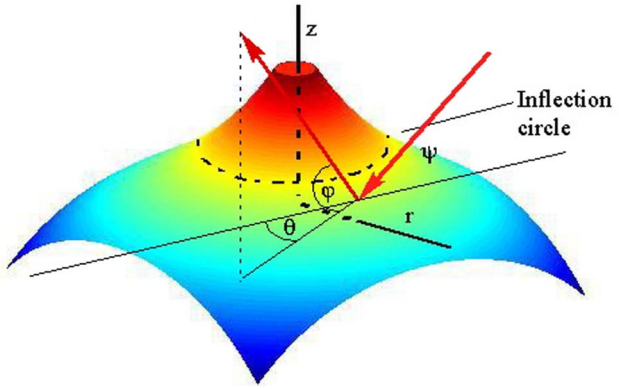

Fig. 5. (Color online) Scattering geometry. ψ, solar elevation angle; θ, azimuthal scattering angle; ϕ, polar scattering angle.

where $\theta_{\max}$ is given by Eq. (24) with

$$\Omega = \{3\ \sin(\psi) + [8\cos^2(\psi) + \sin^2(\xi)]^{1/2}\}/4\sin(\xi). \tag{27}$$

In analogy to the case of arbitrary horizontal incidence, the angle θ of the principal peak of the Airy caustic increases from zero to π or from zero to $\theta_{\max}$ and then decreases back again to zero as ϕ monotonically increases from $-\psi$ to some value less than or equal to $\pi/2$. Again, $d\theta/d\phi = 0$ at $\theta_{\max}$, ensuring that the trajectory of the Airy caustic is smooth at the turnaround point in θ.

The flux tube approach of Subsection 2.D from [1] is again used to determine the intensity along the Airy caustic. After much algebra we obtain

$$\begin{aligned}I_{\text{ref}} = I_{\text{inc}}(r_0/R)[\sin(\epsilon)/(\partial z_0/\partial z')]/\\ [M\cos(\varphi)\cos(\psi)\cos(\xi)\cos(\epsilon)],\end{aligned} \tag{28}$$

where

$$\begin{aligned}M = |(d\theta/d\Omega)[1 + \tan(\phi)\sin(\theta - \epsilon)\tan(\xi)]\\ + (d\phi/d\Omega)\cos(\theta - \epsilon)\tan(\xi)/\cos^2(\varphi)|,\end{aligned} \tag{29}$$

$(d\theta/d\Omega)$ and $(d\phi/d\Omega)$ are obtained by taking the derivatives of Eqs. (23) and (24), and

$$\begin{aligned}(\partial z_0/\partial z') = [1 - \tan(\psi)\tan(\xi)/\\ (1 - b'^2/b'^2_{\max})^{1/2}]/[AB\ \times \cos(\psi)].\end{aligned} \tag{30}$$

It should be noted that both $\sin(\epsilon)$ and $(\partial z_0/\partial z')$ vanish as $\epsilon \to 0$, but that their quotient remains finite and smoothly varying there. Equations (28)–(30) for the reflected intensity are not yet in final form: everything in them is a function only of ϵ, except for $(\partial z_0/\partial z')$, which is a function of $b'/b'_{\max}$, and implicitly of z', since $b'_{\max}$ is a function of z' via Eq. (20). The relation between ϵ and $b'/b'_{\max}$ is

$$\begin{aligned}b'/b'_{\max} = \cos(\epsilon)[1 - \tan^2(\psi)\tan^2(\xi)]^{1/2}/[1\\ + \sin(\epsilon)\tan(\psi)\tan(\xi)].\end{aligned} \tag{31}$$

No further simplification of the arbitrary diagonal incidence intensity was uncovered, so we report Eqs. (28)–(31) as our final form of the intensity.

The shape of the caustic is determined by Eqs. (22) and (24); in Figs. 6(a)–6(c) we plot the scattering angles of the Descartes ray as a function of polar angles (θ, ϕ) for varying values of the solar angle ψ (30°, 36° and 40°). We use a tangent cone angle of 63°, corresponding to the case discussed in Section 3 below.

3. Observation of the Reflection Rainbow from Dewdrops

It is mid-morning on a sunny day and there is still dew on the grass. The solar angle of Eq. (4) is in the range $30° < \psi < 50°$, and the dew hangs as pendant

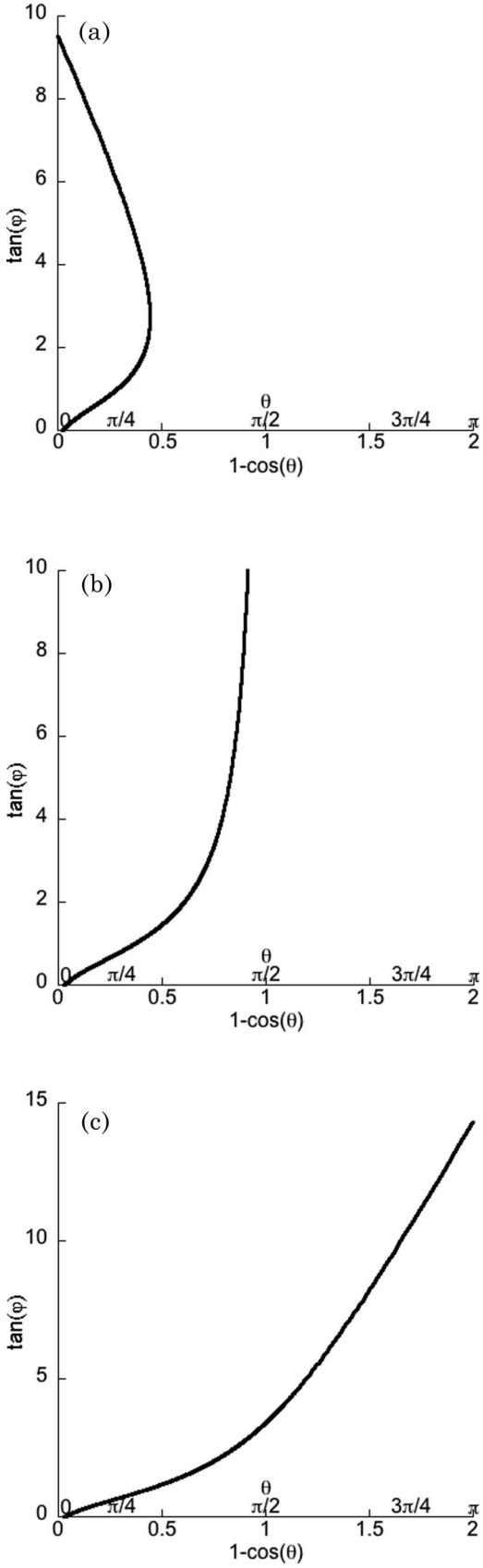

Fig. 6. (Color online) Descartes ray scattering angles at different solar elevations; the tangent cone angle is $\psi = 63°$. Note that for solar elevation angles greater than 36°, the scattering extends to $\theta = 180°$: (a) $\psi = 30°$, (b) $\psi = 36°$, (c) $\psi = 40°$.

droplets of diameter $1\,\text{mm} < d < 2\,\text{mm}$ from the blades of grass. A person observing the pendant dewdrops occasionally sees a bright glare spot of sunlight reflected from a drop as in Fig. 1 as he crouches and looks down on them from a meter or so away. Very rarely, at a scattering angle θ in the horizontal plane in the range $80° < \theta < 120°$, the reflected glare spot appears brightly colored. If one then photographs the colored glare spot with a camera that is greatly misfocused, the glare spot image is a blur circle. Within the blur circle is a rainbow consisting of a principal peak and a number of supernumerary peaks flanking it on one side. The principal peak is white, rather than colored, and the supernumerary fringes are only weakly colored, being blue on the side closer to the principal peak and red on the side farther from it. Alternatively, if one crouches a few centimeters from the droplet and looks down at it with misfocused vision, the same blur circle containing the principal rainbow peak flanked by a series of supernumeraries is again observed.

These observations are qualitatively consistent with the results of Section 2. For the first-order atmospheric rainbow, the scattered electric field is proportional to

$$E_{\text{scattered}}(\theta) \approx \text{Ai}[-k^{2/3}a^{2/3}(\theta - \theta_{\text{Descartes}})/h^{1/3}], \quad (32)$$

where $\theta_{\text{Descartes}}$ and h depend on the refractive index of the water droplet, which in turn depends on the wavelength λ of the incident light [4]. This wavelength dependence is responsible for the bright colors of the principal peak of the atmospheric rainbow. The total absence of the color of the principal peak of the dewdrop rainbow is evidence that it is due to reflection only. The sole wavelength dependence in the reflection rainbow expressions of Eq. (16) is the $k^{2/3}$ factor. This causes the $\text{Ai}(0)$ point to occur at the same angular location for each wavelength [the $\text{Ai}(0)$ point is on the shadowed-side shoulder of the principal rainbow peak] and causes the Airy pattern to be more angularly spread for red light than it is for blue light, in qualitative agreement with observations.

As to observing the reflection rainbow at θ in the vicinity of 90° at a steep value of ϕ as one crouches near the droplet and looks down on it, this corresponds to the case of Eqs. (25) and (26) when $\xi \approx \pi/4 + \psi/2$. For $\psi \approx 36°$ ($\pi/10$ rad, a typical value), one has $\xi \approx 63°$. If the dewdrop hangs from the blade of grass so that it is roughly circularly symmetric, its size is just right so that the tangent cone at the inflection circle has $\xi \approx \pi/4 + \psi/2$, then one can stand somewhere near $\theta = 90°$, look down on the droplet ($\phi \approx 90°$), and see the effect. But what size of droplets is just right? Reference [5] gives the angle of the tangent cone ξ as a function of the variable β [see Eq. (34) below] for $\beta \geq 0.25$, and the horizontal radius at the bottom of the droplet r_H in terms of β. The angle ξ as a function of β is almost exactly a straight line for $0.25 \leq \beta \leq 0.40$. If one extrapolates the graph to $\xi = 45°$, one gets $\beta = 0.19$, and r_H decreases to

1.19 mm. Although extrapolation of the data of [5] to $\xi = 63°$ is unwarranted, the solution must correspond to very small β and r_H less than 1 mm. This is within the range of the estimated sizes of the dewdrops that were observed to produce the effect. The results of Section 1 thus provide a reasonable plausibility argument that the dewdrop observations are in fact an example of the reflection rainbow of a pendant droplet and explain the rarity of the effect seen in mid-morning sunlight.

4. External Reflection Rainbow as a Fluids Diagnostic

As a final comment, measurement of the specular reflection rainbow caustic provides a method for determining the location and radius of the inflection circle of a pendant droplet. Let r_H be the radius of curvature at the bottom of the droplet, ρ and λ be the density and viscosity of water, and g be the acceleration due to gravity. Then the shape of the pendant droplet is given by[2]

$$-(\mathrm{d}^2r/\mathrm{d}z^2)/[1 + (\mathrm{d}r/\mathrm{d}z)^2]^{3/2} + 1/\{r[1 + (\mathrm{d}r/\mathrm{d}z)^2]^{1/2}\} = (2/r_H) - (z\beta/{r_H}^2), \quad (33)$$

where

$$\beta = \rho g {r_H}^2/\gamma, \quad (34)$$

and where the origin of coordinates is taken to be at the bottom of the droplet. Assume that the shape of the droplet surface a small vertical distance δ above or below the inflection circle is given by Eq. (1) of [1] and that δ is small enough that $r_i \gg \delta$, $\delta \ll r_i/\alpha {r_H}^2$, and $\delta \ll 1/r_i\alpha$. Then substitution of Eq. (1) of [1] into Eq. (33) gives

$$\cos(\xi)/r_i = (2/r_H) - (z_0\beta/{r_H}^2), \quad (35)$$

$$\beta/{r_H}^2 - 6\alpha \times \cos^3(\xi) + \sin(\xi)/{r_0}^2 = 0. \quad (36)$$

This suggests a simple means of measuring the fluid parameters r_i and z_i: using an apparatus similar to the one in [1], one can illuminate a pendant droplet with horizontally incident light. Measurement of the direction of the reflection caustic on the viewing screen gives ξ via Eq. (8) of [1], and the measured supernumerary spacing gives α via Eq. (21) of [1]. If, in addition, the radius of curvature of the bottom of the droplet is measured so as to obtain β via Eq. (34), substitution into Eq. (36) gives the radius r_0 of the inflection circle, and then substitution into Eq. (35) gives the height z_0 of the inflection circle above the bottom of the droplet. However, these parameters are determined by the density and surface tension of the droplet [2]. In principle, one can therefore use the information gathered from the external reflection rainbow caustic to determine the surface tension. Current techniques for determination of surface tension involve measurement of the entire profile of the droplet; the technique outlined above may prove simpler and cheaper than the currently used technique.

5. Conclusions

In this sequence of two papers we have developed a mathematical theory for the shape of the external reflection rainbow caustic produced by a pendant droplet; we have also qualitatively demonstrated that this is what is seen in glare spots on dewdrops or guttation drops on grass. It is also likely that one can use the caustic to measure the value of the surface tension of the fluid, as the density, surface tension, and volume of the droplet determine the pendant droplet shape.

The work done in this paper by C. L. Adler was supported by Research Corporation grant CC6308.

References

1. J. A. Lock, C. L. Adler, and R. W. Fleet, "Rainbows in the grass. I. External-reflection rainbows from pendant droplets," Appl. Opt. **47**, H203–H213 (2009).
2. J. F. Padday, "The profiles of axially symmetric menisci," Philos. Trans. R. Soc. London Ser. A **269**, 265–293 (1971).
3. J. F. Nye, *Natural Focusing and Fine Structure of Light* (Institute of Physics, 1999), pp. 10–25.
4. H. C. van de Hulst, *Light Scattering by Small Particles* (Dover, 1981), pp. 240–246.
5. S. Fordham, "On the calculation of surface tension from measurements of pendant drops," Proc. R. Soc. London Ser. A **194**, 1–16 (1948).